Bioactive Materials 21 (2023) 499–510

Contents lists available at ScienceDirect

Bioactive Materials

journal homepage: www.keaipublishing.com/en/journals/bioactive-materials

Transferrin-guided intelligent nanovesicles augment the targetability and potency of clinical PLK1 inhibitor to acute myeloid leukemia

Yifeng Xia [a,b,1], Jingnan An [c,1], Jiaying Li [d], Wenxing Gu [a], Yifan Zhang [a], Songsong Zhao [a], Cenzhu Zhao [c], Yang Xu [c,*], Bin Li [d], Zhiyuan Zhong [a,b,**], Fenghua Meng [a,b,***]

[a] Biomedical Polymers Laboratory, College of Chemistry, Chemical Engineering and Materials Science, and State Key Laboratory of Radiation Medicine and Protection, Soochow University, Suzhou, 215123, PR China
[b] College of Pharmaceutical Sciences, Soochow University, Suzhou, 215123, PR China
[c] Jiangsu Institute of Hematology, The First Affiliated Hospital of Soochow University, Institute of Blood and Marrow Transplantation of Soochow University, Collaborative Innovation Center of Hematology, Soochow University, Suzhou, 215123, PR China
[d] Orthopedic Institute, Soochow University, Suzhou, 215007, PR China

ARTICLE INFO

Keywords:
Polymersomes
Targeted delivery
Acute myeloid leukemia
Polo-like kinase 1
Molecular targeted drug

ABSTRACT

Acute myeloid leukemia (AML) remains a most lethal hematological malignancy, partly because of its slow development of targeted therapies compared with other cancers. PLK1 inhibitor, volasertib (Vol), is among the few molecular targeted drugs granted breakthrough therapy status for AML; however, its fast clearance and dose-limiting toxicity greatly restrain its clinical benefits. Here, we report that transferrin-guided polymersomes (TPs) markedly augment the targetability, potency and safety of Vol to AML. Vol-loaded TPs (TPVol) with 4% transferrin exhibited best cellular uptake, effective down-regulation of p-PLK1, p-PTEN and p-AKT and superior apoptotic activity to free Vol in MV-4-11 leukemic cells. Intravenous injection of TPVol gave 6-fold higher AUC than free Vol and notable accumulation in AML-residing bone marrow. The efficacy studies in orthotopic MV-4-11 leukemic model demonstrated that TPVol significantly reduced leukemic cell proportions in periphery blood, bone marrow, liver and spleen, effectively enhanced mouse survival rate, and impeded bone loss. This transferrin-guided nano-delivery of molecular targeted drugs appears to be an interesting strategy towards the development of novel treatments for AML.

1. Introduction

Acute myeloid leukemia (AML) remains one of the most lethal hematological malignancies [1]. AML is characterized by lacking specific antigens, which hinders the clinical development of targeted therapies such as antibodies, antibody-drug conjugates, and CAR-T cell therapy [2]. It is reported that ca. 40% remitted AML patients would eventually relapse and become refractory to treatments [3]. The advancement of molecular targeted drugs has revolutionized the therapeutic scheme for various hematological and solid tumors [4,5], as they possess not only better specificity and anti-cancer activity but also less off-target toxicity than traditional chemical agents [6,7]. The analyses of clinical AML samples have shown that 60% AML patients overexpress polo-like kinase 1 (PLK1) [8], for which a variety of PLK1 inhibitors such as volasertib (Vol) and onvansertib have been designed and clinically investigated for treating AML patients [9,10]. Notably, Vol as a lead agent has demonstrated significant clinical efficacy in AML patients [11,12] and has been granted breakthrough therapy status by FDA. However, as most small molecular drugs, Vol suffers from fast clearance, low bioavailability, and frequent and high dosing that induce dose-limiting toxicities such as

Peer review under responsibility of KeAi Communications Co., Ltd.
* Corresponding author.
** Corresponding author. Biomedical Polymers Laboratory, College of Chemistry, Chemical Engineering and Materials Science, and State Key Laboratory of Radiation Medicine and Protection, Soochow University, Suzhou, 215123, PR China.
*** Corresponding author. Biomedical Polymers Laboratory, College of Chemistry, Chemical Engineering and Materials Science, and State Key Laboratory of Radiation Medicine and Protection, Soochow University, Suzhou, 215123, PR China.
E-mail addresses: yangxu@suda.edu.cn (Y. Xu), zyzhong@suda.edu.cn (Z. Zhong), fhmeng@suda.edu.cn (F. Meng).
[1] These authors contribute equally to this work.

https://doi.org/10.1016/j.bioactmat.2022.08.032
Received 8 March 2022; Received in revised form 24 August 2022; Accepted 28 August 2022

megakaryocyte dysmaturity and severe thrombopenia, thus greatly restraining clinical benefits [13].

Targeted delivery with nanomedicines provides a potential strategy for improving the efficacy of molecular drugs [14,15]. Many cancers including AML are found expressing high levels of transferrin receptor, which has stimulated the development of various transferrin-guided nanosystems [16]. Chang et al. reported that anti-transferrin receptor single-chain antibody fragment-mediated nanodelivery of tumor suppressor gene p53 could target metastatic lesions and induce clinical anticancer effects [17]. Unlike antibodies and antibody fragments, transferrin as an endogenous protein is not immunogenic. Huang et al. reported that transferrin conjugated lipopolyplex nanoparticles could significantly increase the therapeutic effect of decitabine and showed excellent potential in AML treatment [18]. It is extremely challenging, nevertheless, to prepare transferrin-guided systems for molecular targeted drugs like Vol because few vehicles can stably load Vol and allow post-modification with transferrin.

Here, we report that transferrin-guided polymersomes (TPs) markedly augment the targetability, potency and safety of Vol to AML (Scheme 1). The chimaeric polymersomes with dithiolane-functionalized polycarbonate as membrane, poly(ethylene glycol) as outer shell and poly(aspartic acid) as inner shell were shown to efficiently encapsulate and deliver Vol to ovarian cancers [19]. Transferrin was conjugated to Vol-loaded polymersomes with controlled density via click chemistry. Notably, PVol with 4% transferrin (TPVol) exhibited best cellular uptake, effective down-regulation of p-PLK1 and p-PTEN, and significant survival benefits in highly malignant MV-4-11 leukemic model. Transferrin-targeted delivery of clinical PLK1 inhibitor appears to be an attractive strategy for treating AML.

2. Experimental section

2.1. Preparation of volasertib-loaded transferrin-guided polymersomes (TPVol)

TPVol was prepared by post-modification of azide-functionalized polymersomal Vol (N_3-PVol) with DBCO modified transferrin (Tf-DBCO) via click chemistry. To prepare N_3-PVol, 100 μL DMSO solution of PEG-P(TMC-DTC)-PAsp (as reported in Ref. [20]) (40 mg/mL), N_3-PEG-P(TMC-DTC) (as reported in Ref. [21]) (2–8 mol% with respect to PEG-P(TMC-DTC)-PAsp), and volasertib (Vol, 4 mg) was added under stirring into HEPES buffer (pH 6.8, 5 mM, 0.9 mL). The resulting dispersion was incubated at 37 °C for 2 h in a shaking bath (200 rpm) and then dialyzed against HEPES (pH 7.4, 5 mM) for 6 h (MWCO 14000 Da).

To prepare Tf-DBCO, 41 μL of DBCO-OEG_4-NHS solution (10 mg/mL) in DMSO was added into 2 mL of Tf solution (20 mg/mL) in MiliQ water (Tf/DBCO molar ratio of 1/1.2) followed by reaction at 37 °C in shaking bath (200 rpm). After 12 h, the mixture was subject to ultrafiltration (MWCO 10 kDa) for 3 times. The final Tf concentration was determined by BCA kit, and the DBCO functionality of Tf-DBCO was determined by MALDI-TOF mass spectrometry.

TPVol was prepared by adding freshly prepared Tf-DBCO into N_3-PVol solution at a Tf-DBCO/N_3 molar ratio of 1.8/1 under stirring, reacting for 12 h under shaking (100 rpm, 37 °C), and purified via ultrafiltration (Millipore, MWCO 1000 kDa). The non-targeted formulation, PVol, was prepared similarly as for N_3-PVol from PEG-P(TMC-DTC)-PAsp and Vol. The size distribution and Vol loading content of TPVol and PVol were determined. The morphology of PVol was determined by cryo-TEM. The stability of TPVol and PVol at 4 °C, against 10% FBS, or under 10 mM GSH was monitored using DLS. Besides determination using BCA protein assay kit, the Tf content on TPVol was also quantified using fluorometry. Briefly, TPVol with unknown Tf content was incubated with excess rabbit anti-human Tf antibody for 15 min followed by twice centrifugal ultrafiltration (MWCO: 1 MDa). Then Alexa Fluor™ 647-labeled goat anti-rabbit IgG secondary antibody was added to incubate for 15 min following the same purification procedure. Then polymersome solution was 20-fold diluted to measure the fluorescence intensity. The Tf content on TPVol could be determined based on a standard curve of Alexa Fluor™ 647-labeled secondary antibody.

2.2. Hemolytic analysis

Mouse blood (2 mL) was washed three times with 8 mL sterile PBS.

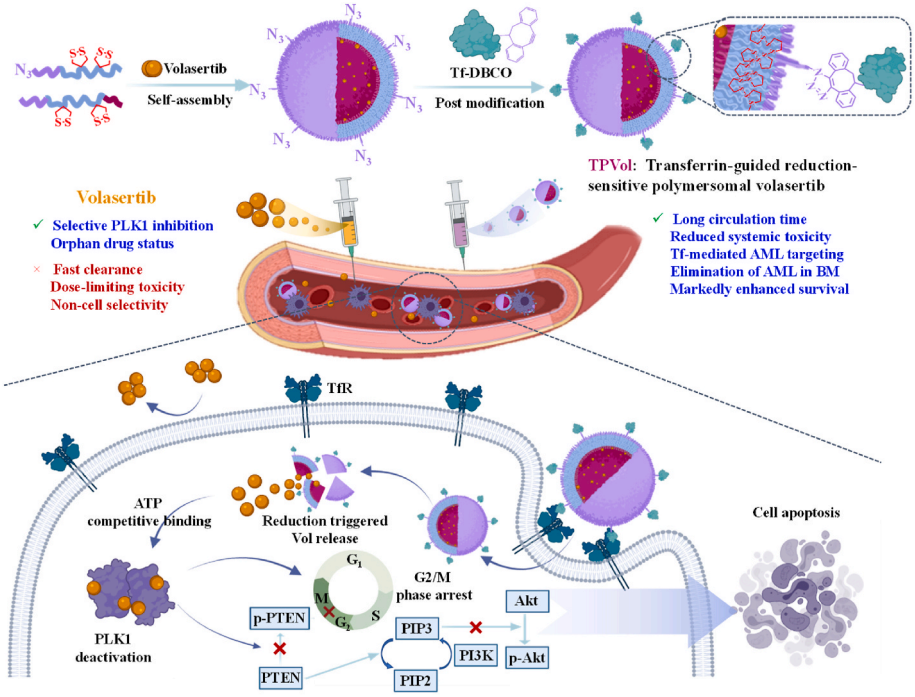

Scheme 1. Illustration of preparation of transferrin-decorated polymersomal volasertib (TPVol) and its targeted delivery and cytoplasmic release of volasertib to AML cells.

The red cell suspensions after 9-fold dilution with sterile PBS were incubated for 3 h with TPVol, PVol or Vol solutions (Triton solution and pure water as positive controls) and centrifuged at 150×*g* for 5 min. The supernatants were taken for UV–vis measurements (at 545 nm).

2.3. Transferrin receptor (TfR) expression on AML cell lines and patient primary cells

Bone marrow (BM) samples were collected from four AML patients for determining TfR expression and the effect of TPVol on cell growth inhibition and apoptosis of primary cells, which were approved by the ethics committee of the First Affiliated Hospital of Soochow University (Suzhou, P.R. China) in accordance with the Declaration of Helsinki protocol.

To determine the TfR expression, patient primary cells and AML cell lines (MV-4-11, U937) and ALL-697 in EP tubes (5×10^4 cells) were washed (PBS, × 2), resuspended in 100 μL PBS, and stained with APC anti-TfR antibody for 15 min under dark at room temperature. 300 μL PBS was added before flow cytometry analysis (10,000 cells were gated) and MV-4-11 cells without staining were set as negative control.

2.4. Cell apoptosis and cell cycle arrest of TPVol

To evaluate the apoptotic activity, MV-4-11 cells, U937 cells and AML primary cells with high TfR expression (#20210618) and low TfR expression (#20200903 and #20210816) seeded in 6-well plates (3×10^5 cells/well) were incubated with TPVol, PVol or free Vol (Vol conc.: 0.07 μg/mL) for 48 h. The cells were centrifuged, washed, and resuspended in binding buffer before staining with annexin V-Alexa Fluor 647/propidium iodide (PI) under dark for 15 min. Finally, 400 μL binding buffer was added and the cells were measured using flow cytometry.

To investigate cell cycle arrest, MV-4-11 cells in 24-well plates (2×10^5 cells/well) were added with TPVol, PVol or free Vol (Vol conc.: 0.07 μg/mL). After incubation for 48 h, cell cycle kit (Fcmacs) was applied and subject to flow cytometry measurement and analysis using FlowJo software.

2.5. Cell growth inhibition of AML patient primary cells by TPVol

The growth inhibition of patient primary cells was evaluated using trypan blue rejection method. The primary cells with high TfR expression (#20210618) and low TfR expression (#20200903 and #20210816) were cultured in 96-well plates (1×10^5 cells/well). Then 20 μL TPVol, PVol or Vol was added (Vol conc.: 0.1 μg/mL) and cultured for 48 h. Trypan blue solution (0.4%) was added to stain the dead cells, and the cells were observed and counted under an inverted microscope.

2.6. Pharmacokinetics

All animal experiments were approved by the Animal Care and Use Committee of Soochow University (P.R. China), and all protocols conformed to the Guide for the Care and Use of Laboratory Animals. FITC-labeled Vol (Vol-FITC) was prepared by amidation reaction [22], and loaded into polymersomes for studying the pharmacokinetics. PVol-FITC or TPVol-FITC (Vol: 6 mg/kg (mpk), FITC: 0.8 mpk) in 200 μL PB was intravenously injected into healthy Balb/c mice via tail veins (n = 3). At preset time points, ca. ~70 μL blood was withdrawn, treated and analyzed as reported [23] and detailed in supporting information.

2.7. In vivo targeting and fluorescence imaging

To build orthotopic MV-4-11-Luc-GFP AML mouse model, six-week-old female NSG mice (22–24 g) were irradiated with 175 cGy X-ray and 6 h later intravenously injected with 0.02 mL of MV-4-11-Luc-GFP cells (1×10^5). The AML progression was monitored using *in vivo* imaging system on day 6 and 12 post tumor inoculation and the AML infiltration into the major organs and bone marrow were evaluated using flow cytometry.

To assess the targetability and biodistribution of TPVol in orthotopic AML model, on day 13 after tumor inoculation, a single injection of Cy5-labeled TPVol or PVol in 200 μL PB was *i.v.* administrated (Vol: 6 mpk, Cy5: 0.05 mpk). After 8 h, major organs and limb bones of the mice were collected and *ex vivo* imaged using IVIS system (Living Image 2.6 software).

2.8. In vivo anti-AML efficacy in orthotopic MV-4-11 model

The orthotopic AML model was established as above and 5 days after tumor inoculation the bioluminescence was ca. 5×10^5 p/sec/cm^2/sr, the mice were divided into six groups (n = 7) and the day was denoted day 0. On day 0, 2, 4 and 6, free Vol, PVol, 2%TPVol, 4%TPVol (dose: 6 mpk) and PBS were *i.v.* injected. For 4%TPVol, we also adopted a different dosing regimen, in which 4%TPVol was *i.v.* administrated on day 0, 3, 6 and 9 at a dose of 9 mpk. The body weight was monitored every two days and normalized to the initial weight on day −1. On day 0, 3, 6 and 9, the mice were *in vivo* imaged to track the tumor progression using IVIS imaging system. The survival curves of mice were recorded, and those with body weight loss over 15% were also consider dead.

2.9. Flow cytometry, histological and μCT analyses of mice treated with Vol formulations

The AML mice were treated with PBS, free Vol, PVol, or 4%TPVol (6 or 9 mpk) as described above (n = 3). On day 9 the mice were sacrificed and peripheral blood (PB), liver, spleen, hind femur and tibia were collected for AML cell infiltration and histological analysis. To determine the AML cell infiltration, PB, part of liver, spleen, and hind limbs were grinded and filtrated to get cell suspension. The cells were centrifuged (600×*g*, 5 min) and treated with 5 mL ACK lysis buffer at 4 °C for 5 min and terminated with 10 mL PBS. The cells were then labeled using anti-CD45-APC for flow cytometric analyses. Moreover, aliquots of cells collected from bone marrow were subject to lysis by ice-cold RIPA buffer for western blot measurements for the expression of PLK1, p-AKT, AKT using GAPDH as reference protein (supporting information), and the gels were further semi-quantified using ImageJ software.

The μCT (SkyScan 1176, Belgium) was used to measure and quantitatively analyze hind femurs and tibias using NRecon software. The slices of main organs and leg bones were stained with tartrate resistant acid phosphatase (TRAP, Servicebio, China) and observed using Olympus BX41 microscope for determining tissue damage, leukemic infiltration and osteoclast formation.

2.10. Statistical analysis

Data were expressed as mean ± s.d. Differences among groups were evaluated using one-way Anova and Tukey multiple comparison test or student *t*-test. Survival curves were evaluated using Kaplan-Meier and log-rank comparison test using Graphpad Prism 8. *$p < 0.05$ was significant, and **$p < 0.01$, ***$p < 0.001$, ****$p < 0.0001$ highly significant.

3. Results and discussion

3.1. Preparation of TPVol

Lack of potent and safe molecular targeted drugs is one of the main reasons for little survival improvement of AML patients over the past decades. Here, targeted delivery of clinical PLK1 inhibitor, Vol, was proposed as a novel strategy to enhance the efficacy as well as safety of targeted molecular therapy for AML. The disulfide-crosslinked

chimaeric polymersomes are one of the few systems that could stably load Vol [19]. To target AML, we further modified Vol-loaded polymersomes (PVol) with transferrin by click chemistry. Firstly, Vol-loaded azide-functionalized polymersomes (N_3-PVol) were prepared via co-self-assembly of N_3-PEG-P(TMC-DTC) (7.5-(15.0–2.0) kg/mol) and PEG-P(TMC-DTC)-PAsp (5.0-(15.0–2.0)-1.29 kg/mol) at a molar ratio of 2/98, 4/96, 6/94 or 8/92 with Vol (9.1 wt%) in HEPES buffer. All N_3-PVol showed a good Vol loading content (ca. 5.2 wt%), small size (46.3–48.2 nm), and narrow size distribution (PDI = 0.11–0.13) (Table S1). The cryo-TEM image of PVol showed uniform vesicular morphology (Fig. S1). Then, TPVol was prepared through post-modification of N_3-PVol with DBCO-functionalized transferrin (Tf-DBCO) via click chemistry. Tf-DBCO was synthesized by treating Tf with DBCO-OEG$_4$-NHS at a fixed Tf/DBCO molar ratio of 1/1.2, which yielded quantitative functionalization, as revealed by MALDI-TOF mass spectrometry measurements (Fig. 1A). BCA assays showed that TPVol was obtained with controlled Tf molar contents of 2%, 4%, 6% and 8% at a fixed Tf-DBCO/N_3 molar ratio of 1.8/1. In addition, Tf content on TPVol was also measured using specific binding with Tf antibody followed by Alexa Fluor™ 647-labeled secondary antibody. From the bound fluorescence intensity of the polymersomes, Tf content could be determined based on a calibration curve (Fig. S2). The results were very close to the theoretical values (2%, 4%, and 6%), confirming successful Tf post-modification via click chemistry. Notably, Tf modification had little influences on size, size distribution and Vol loading content (Table 1, Fig. 1B). Non-targeted control, PVol, which assembled from only PEG-P(TMC-DTC)-PAsp and Vol, had comparable characteristics to TPVol.

The stability and cytotoxicity studies with 4%TPVol displayed that TPVol was stable with little size change in PBS under 10% FBS at 37 °C or over 7 days storage at 4 °C (Fig. 1C), and maintained the same cytotoxicity toward MV-4-11 leukemic cells after 7-day storage (Fig. 1D). However, under 10 mM GSH, TPVol was quickly destabilized (Fig. 1E), in line with a fast reduction-responsivity of DTC-based nanosystems [24]. Fig. 1F shows that TPVol and PVol caused significantly less hemolysis than free Vol and pure water, indicating excellent biocompatibility. MTT assays in L929 fibroblasts revealed that both TPVol and PVol were essentially non-toxic at a concentration of 40 μg Vol equiv./mL, whereas free Vol caused significant cytotoxicity (Fig. 1G). These results support that TPVol has favorable properties and is less cytotoxic to normal cells than free Vol.

Table 1
Characterization of TPVol obtained by post-modification at a Tf-DBCO/N_3 molar ratio of 1.8/1.

Entry	N_3 Surface Density (mol.%)	Size[a] (nm)	PDI[a]	DLC[b] (wt. %)	DLE[b] (%)
1	2	48.1 ± 0.8	0.14 ± 0.03	5.0	52.1
2	4	48.9 ± 0.9	0.15 ± 0.02	4.9	51.2
3	6	49.4 ± 1.1	0.16 ± 0.03	5.1	53.5
4	8	50.9 ± 1.3	0.16 ± 0.02	4.9	52.0

[a] Measured by DLS using a Zetasizer Nano-ZS at 25 °C in PB (10 mM, pH 7.4).
[b] Determined by UV-vis measurements.

3.2. *In vitro cellular uptake, cytotoxicity and blockage of PLK1 signaling*

Transferrin receptors (TfR) are overexpressed on several malignant tumors in patients, and TfR-targeting nano-formulations have advanced to clinical trials for treating lung, breast and ovarian cancers [25,26]. TfR was also found highly upregulated in AML cells [18], and 57% AML patients overexpress TfR [27]. FACS analyses confirmed that MV-4-11 and U937 cell lines have high TfR expression while low TfR expression was observed on 697 cells (Fig. 2A). Cellular uptake studies using Cy5-labeled TPVol and PVol showed clearly enhanced internalization of TPVol by MV-4-11 cells and TPVol with 4% Tf appeared to be the best (Fig. 2B). CLSM images and semi-quantitative analyses of fluorescent intensity revealed that the internalization of 4%TPVol was ca. 3-fold that of PVol (Fig. S3). TPVol presenting an optimal Tf density at 4%, which is in agreement with previous report [29]. This is possibly because further increase of Tf density would increase non-specific interactions with serum proteins thereby reducing targeting ability, or bind too strongly to leukemic cells hindering cell internalization. Accordingly, cytotoxicity studies showed that all TPVol caused better inhibitory activity to MV-4-11 cells than PVol and free Vol, and 4% TPVol possessed the highest potency (Fig. 2C). The IC_{50} of 4%TPVol was 0.07 μg/mL, which was ca. 2 and 3-fold lower than that of PVol and Vol, respectively. The targeting ability of 4%TPVol was also verified in TfR

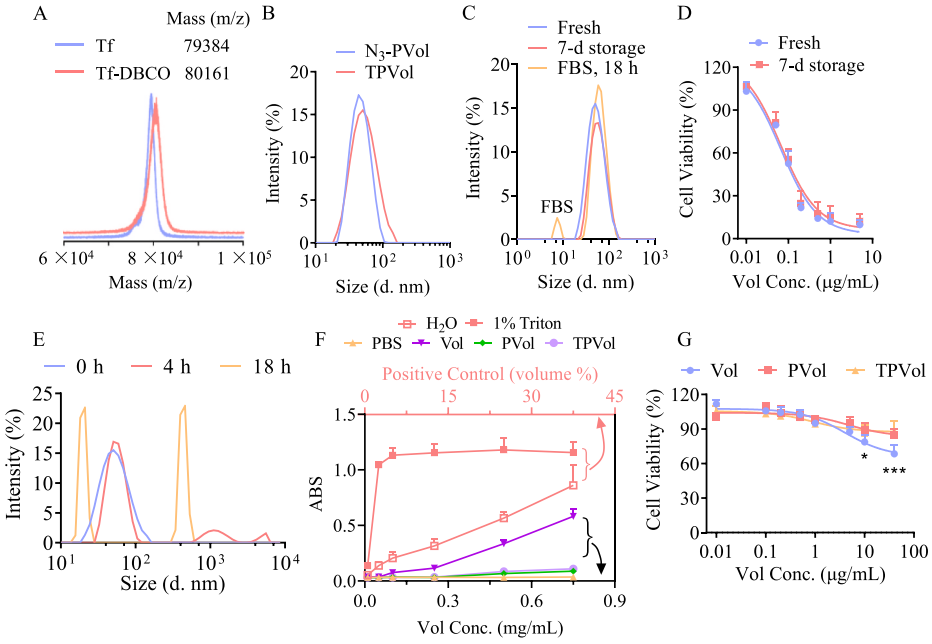

Fig. 1. (A) MALDI-TOF mass spectrometry of Tf and Tf-DBCO. (B) Size distribution of TPVol and N_3-PVol. (C) Stability of TPVol over 7-day storage at 4 °C or 10% FBS at 37 °C. (D) The viability of MV-4-11 cells after 72 h incubation with freshly made or stored TPVol. (E) Size change of TPVol in response to 10 mM GSH at 37 °C. (F) Hemolysis assay of mouse hemocytes after 3 h incubation with free Vol, PVol and TPVol. Pure water and Triton solution were as positive controls. (G) Cell viability of L929 fibroblasts following 4 h incubation with free Vol, PVol and TPVol and subsequent 68 h culture with drug-free medium. Statistical analysis: one-way ANOVA with Tukey multiple comparisons tests: *p < 0.05, ***p < 0.001, ****p < 0.0001.

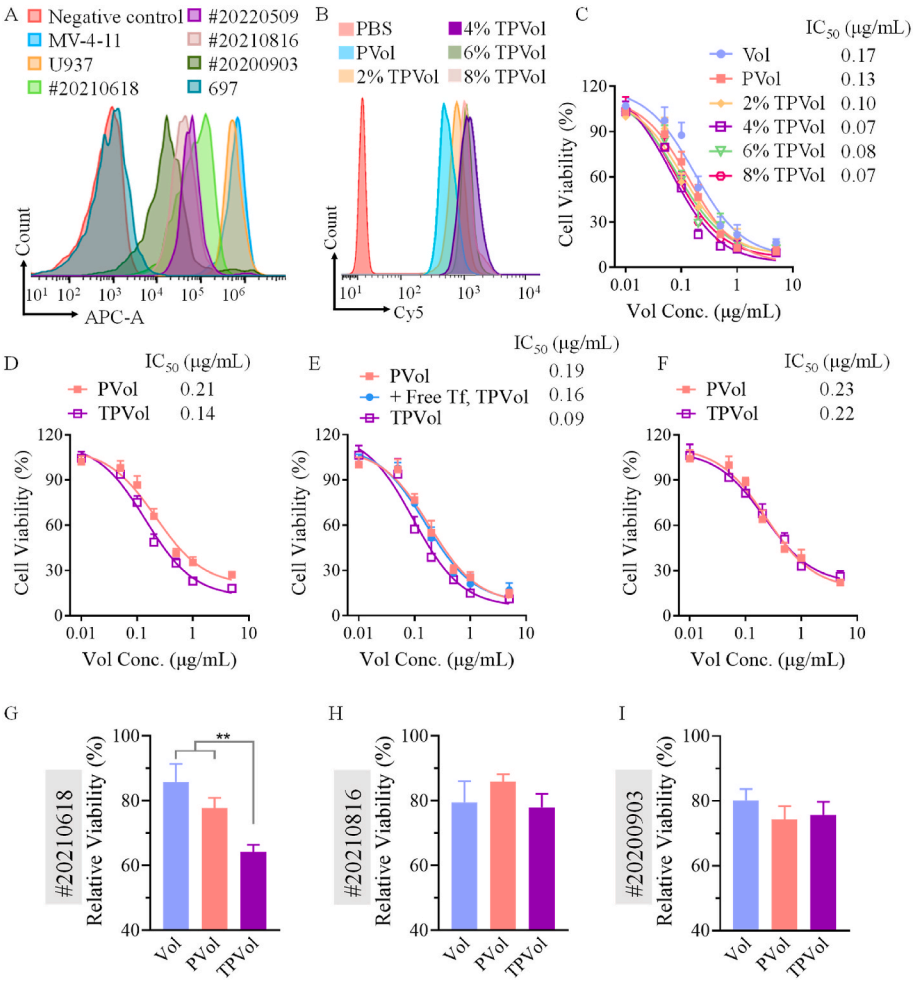

Fig. 2. TfR expression of cells, and cellular uptake and cytotoxicity studies of TPVol. (A) TfR expression on AML cell lines (MV-4-11, U937 and 697 cells) and AML patient primary cells (#20210618, #20220509, #20210816 and #20200903) determined using TfR antibody by flow cytometry. (B) Uptake of Cy5-labeled PVol or TPVol with different Tf surface contents by MV-4-11 cells at 2-h incubation. MTT assays of TPVol in MV-4-11 cells (C), U937 cells (D), Tf-pretreated MV-4-11 cells (E), and ALL-697 cells (F). Growth inhibition of AML patient primary cells with (G) TfR overexpressing (#20210618) and (H&I) TfR low-expressing (#20210816 and #20200903) at 48-h treatment with TPVol, PVol or Vol (Vol conc.: 0.1 μg/mL).

overexpressing U937 cells (Fig. 2D). For the inhibition experiments, in free Tf-pretreated MV-4-11 cells as well as in TfR low-expressing 697 cells, TPVol exhibited similar inhibitory activity to PVol (Fig. 2E and F). These results confirm the active targeting effect of TPVol toward MV-4-11 cells via TfR-mediated endocytosis, and Tf density plays an important role [28,29].

The apoptosis studies further revealed that TPVol and PVol treatment provoked 77.8% and 54.7% apoptosis of MV-4-11 cells, respectively, which were significantly higher than that for free Vol (14.9%) (Fig. 3A). Similar results were also observed in U937 cells (Fig. S4). The cell cycle assay displayed that TPVol induced obviously more cell arrest in G2/M phase than PVol and Vol (83% vs 61% and 45%) (Fig. 3B), illustrating the strong effect of PLK1 inhibition on cell cycle. PLK1 as a serine/threonine protein kinase is a master regulator of cell cycle progression, controls G2/M checkpoint [30,31], and is essential for tumor growth, such as DNA damage response. Using PLK1 as the target, onvansertib received FDA approval for treating KRAS mutant mCRC [32]. PLK1 expression was found high in several malignant cancers including AML [33–36]. The inhibition of PLK1 by volasertib would result in blocking of cell division and ultimately cell apoptosis [37]. We then evaluated the effect of Vol formulations on PLK1 signaling pathway in MV-4-11 cells (Fig. 3C&D). Western blot results disclosed that PLK1 expression had no big difference among groups, while p-PLK1 was significantly downregulated by TPVol indicating its strong deactivation effect against PLK1. The greatly increased CDC25 expression of TPVol treated cells was in line with the results of cell cycle arrest. Vol was reported to be a ATP-competing PLK inhibitor by binding the ATP-binding pocket of human PLK1 protein, leading to blockage of PLK1 signaling pathway and cell apoptosis [38]. PLK1 inhibitor could significantly inhibit the PTEN phosphorylation that was triggered by PLK1 [39], whereas PTEN as a negative regulator of oncogenic PI3K-AKT signaling could block the activation and the phosphorylation of AKT [40], thus resulting in upregulation of AKT and downregulation of p-AKT. PI3K-AKT pathway is crucial for cell proliferation and associated with the activation of PLK1 in mitotic cells [41]. WB results displayed that among all groups, TPVol treatment exhibited the most increased PTEN expression and decreased p-PTEN expression, as well as significantly down-regulated p-AKT, confirming our hypothesis (Scheme 1). Collectively, enhanced cellular uptake of TPVol in TfR overexpressing cancer cells results in further downregulation of p-AKT and thereby augmented cytotoxicity and apoptosis compared to PVol and free Vol.

The anti-leukemic activity of TPVol was also studied in AML patient primary cells (Table S2) with various levels of TfR expression (Fig. 2A). The results showed that TPVol induced significantly more apoptosis of TfR overexpressing primary cells (#20210618) than PVol and free Vol, while in TfR low-expressing cells (#20210816 and #20200903) TPVol exhibited comparable apoptotic activity to free Vol (Fig. 2G, H&I, Fig. S5). The enhanced anti-leukemic activity of TPVol in TfR overexpressing primary cells was further confirmed by trypan blue rejection assays, indicating clinical relevance of TPVol.

3.3. *Pharmacokinetics and biodistribution of PVol and TPVol in mice*

Encouraged by the excellent performance of TPVol *in vitro*, we then investigated the *in vivo* pharmacokinetics of TPVol in healthy Kunming mice using FITC-labeled Vol (Vol-FITC) as a model drug. Fig. 4A shows

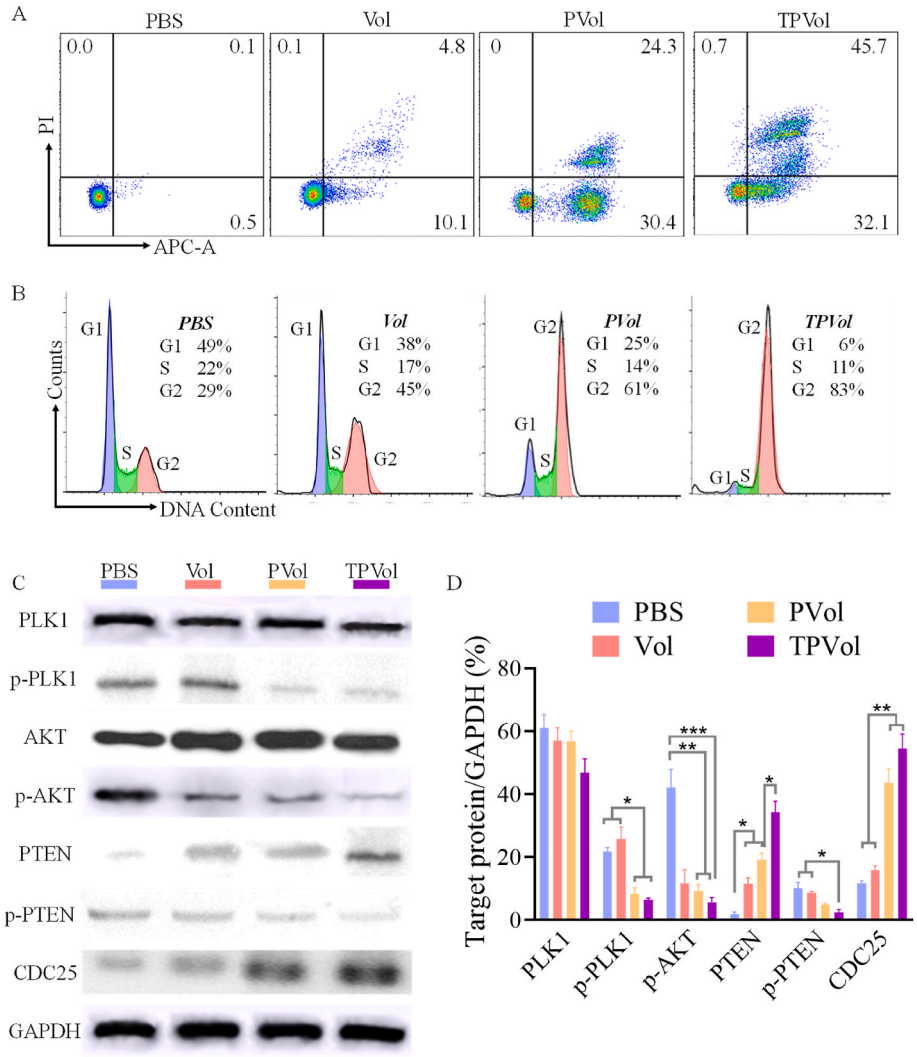

Fig. 3. The apoptosis assay (A), cell cycle assay (B) and western blot measurement (C, D) of MV-4-11 cells following 48-h incubation with free Vol, PVol or TPVol (Vol Conc: 0.07 μg/mL). Statistical analysis: one-way ANOVA with Tukey multiple comparisons tests: *p < 0.05, **p < 0.01, ***p < 0.001.

that free drug was cleared rapidly showing an elimination half-life ($t_{1/2,\beta}$) of 2.5 h. While PVol and TPVol circulated prominently longer with $t_{1/2,\beta}$ of 12.9 and 10.7 h, respectively. The significantly increased AUC of PVol and TPVol compared with free Vol (Fig. 4B) illustrates the effective protection of Vol by polymersomes and little negative influence of Tf on the blood circulation of polymersomes. The longer circulation time compared with CD44-targeting polymersomes [42] may be attributed to the lower surface density of targeting ligands.

To investigate the tumor accumulation and anti-AML performance of TPVol *in vivo*, we built orthotopic AML model in NSG mice by irradiation with 175 cGy X-ray and 6 h later intravenous (*i.v.*) injection of MV-4-11-Luc-GFP cells (1×10^5). The *in vivo* imaging showed that MV-4-11-Luc-GFP cells significantly infiltrated into bone marrow as from day 6 (Fig. 4C). The proportion of MV-4-11-Luc-GFP cells became very prominent on day 12, reaching 57.8%, 12.4% and 7.3% in BM, liver and spleen, respectively (Fig. 4D). This engraftment of MV-4-11 cells in the BM corroborates successful building of AML mouse model [43], as homing of leukemic cells in the BM is characteristic of AML patients [44]. Using such model, the accumulation of TPVol and PVol in the BM was visualized at 8 h post injection of Cy5-labeled TPVol or PVol. The *ex vivo* images of hind femurs and tibias and quantitative analyses (Fig. 4E and F) revealed significantly more TPVol than PVol in the BM (**p). Similar findings were reported in CD44-targeting polymersomes, indicating the potential of such polymersomes in AML treatment [45]. Moreover, TPVol group showed higher Cy5 fluorescence in BM than in other major organs (Fig. 4G), while liposomes with dual targeting ligands showed more accumulation in kidney and lung compared with bone marrow [46]. There was no much difference between TPVol and PVol in main organs, possibly due to the relatively low infiltration of AML cells other than BM. This enhanced accumulation of TPVol in the limb bones is likely a result of bone-homing feature of MV-4-11 cells (Fig. 4D) combined with targeting effect of TPVol to MV-4-11 cells.

3.4. *In vivo* therapeutic effect of TPVol in orthotopic AML model

To study the anti-AML performance of TPVol in orthotopic MV-4-11-Luc-GFP leukemic mice, on day 5 post-implantation of AML cells, free Vol, PVol, TPVol at 6 mpk or PBS was *i.v.* administrated every 2 days (Fig. 5A). The progression of MV-4-11-Luc-GFP tumor was monitored by using *in vivo* imaging. Fig. 5B shows that as compared to PBS group that had a quick augmentation of tumor bioluminescence and accumulation of leukemic cells in leg bones, all Vol formulations could repress tumor progression though to varying extents. Interestingly, PVol induced significantly better retardation of tumor progression than free Vol at 6 mpk (*p) and Tf targeting further enhanced the inhibitory effect (*p) (Fig. 5B&C). TPVol with 2% and 4% Tf exhibited similar anti-AML activity, in line with previous reports that 3.9% Tf density achieved optimal targeting effect [29]. Fig. 5D displays that PBS group gradually

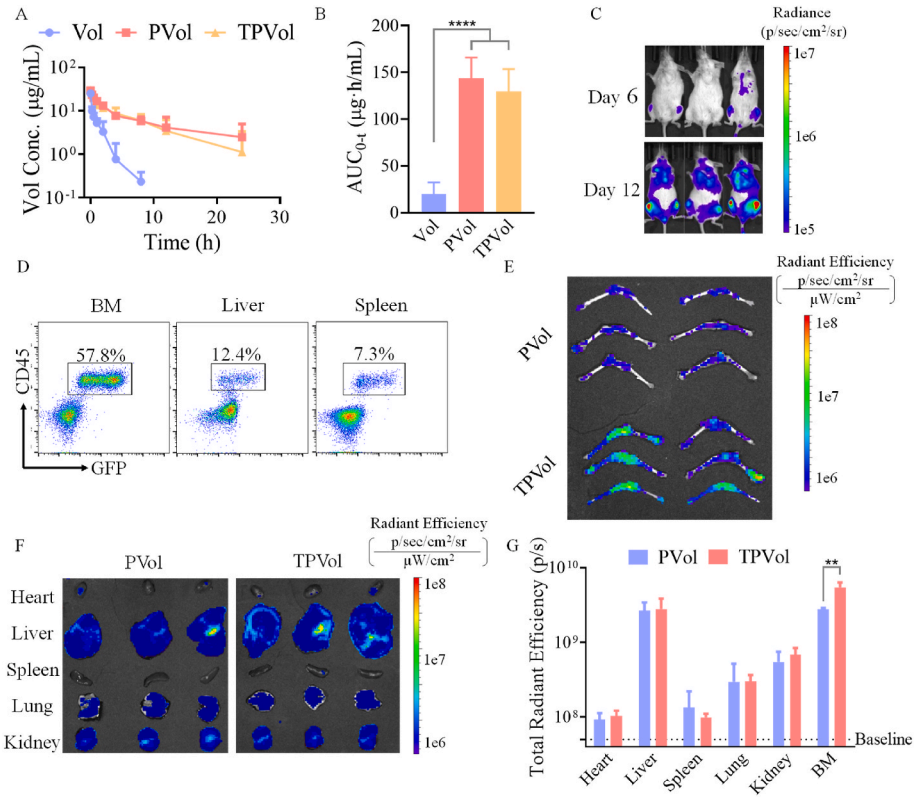

Fig. 4. Pharmacokinetics and biodistribution of TPVol and PVol (Vol: 10 mpk, n = 3). Blood circulation (A) and AUC (B) of FITC-labeled Vol, PVol and TPVol in healthy Balb/c mice. (C) *In vivo* bioluminescence images of NSG mice after i.v. injecting of MV-4-11-Luc-GFP cells on day 6 and 12, and (D) leukemia infiltration in bone marrow (BM), liver, and spleen on day 12. *Ex vivo* images of hind femurs and tibias (E) and main organs (F) at 8 h after injection of Cy5 labeled TPVol or PVol (day 12). (G) The semi-quantitative analyses of TPVol and PVol biodistribution. Statistical analysis: one-way ANOVA with Tukey multiple comparisons tests: **p < 0.01.

lost body weight as a result of aggressive expansion of leukemic cells. In comparison, all Vol groups exhibited barely any body weight loss over the period of treatments, supporting effective suppression of tumor growth as well as little toxic effects of Vol formulations. It should be noted that human Tf was used in this study and how human Tf binds to mouse TfR expressed on the healthy organs and cells remained unclear. Whether the above toxicity results could reflect the situation in human requires further investigation. MV-4-11 leukemia is an extremely malignant model, displayed short median survival time (MST) of 9 days (Fig. 5E). Free Vol and PVol at 6 mpk increased the MST to 12 and 15 days, respectively. Strikingly, both TPVol prolonged the MST to 22 days, which was significant improvement compared with PVol (**p) and highly significant over free Vol (***p) and PBS (***p). The above results confirm that TPVol possesses prominent targetability, enhanced anti-cancer potency, and good safety in MV-4-11-Luc-GFP leukemic model.

The anti-AML effect of 4%TPVol was further investigated at an increased dose of 9 mpk given every 3 days for total four injections. The results revealed markedly enhanced repression of tumor growth compared to TPVol at 6 mpk (*p) without causing apparent toxicity (Fig. 5B, C, D). Accordingly, the MST of MV-4-11-Luc-GFP leukemic mice was extended from 22 days at 6 mpk to 32 days (*p), which was 2.5 longer than PBS (MST = 9 days) (Fig. 5E). This improvement of survival benefits was also significant compared with recent reports with repeated administration of DD8/9 inhibitor and peptidomimetic MYB:CBP inhibitor for malignant leukemic models [47,48]. It should further be noted that unlike free Vol which induced bleeding at the injection site and required several minutes of pressing to stop bleeding, as a result of its platelet depleting effect and dose-limiting toxicity [49], TPVol and PVol stopped bleeding after 2–5 s of pressing. Hence, TPVol provides a novel dually targeted molecular therapy for AML, which not only remarkably improves the therapeutic effect and survival benefits but also reduces systemic toxicities.

3.5. *Ex vivo* evaluation of leukemia blast infiltration, PLK1 regulation and bone damage

To further investigate their anti-AML performance, we evaluated the effect of different Vol formulations on leukemia blast infiltration in BM and main organs, PLK1 regulation and bone damage of MV-4-11-Luc-GFP leukemic mice. The engraftment of MV-4-11-Luc-GFP leukemia blasts in the liver, spleen, BM and peripheral blood (PB) on day 9 was determined using FACS. Fig. 6 shows that PBS group had substantial proportions of leukemia blasts in BM (76.4%), liver (36.7%) and PB (9.1%), which were all dramatically reduced by treatments with Vol formulations. At the same dose of 6 mpk, TPVol resulted in considerably lowered proportions of AML cells in liver, spleen, BM and PB than PVol and free Vol. At an increased dose of 9 mpk, TPVol gave rise to barely detectable leukemia cells in liver, spleen, BM and PB. This effective mitigation of leukemia cells in the BM niche by TPVol is of particular importance, as most anti-AML therapies failed due to their inferior access to BM [43,50,51].

H&E staining images were taken to visualize the infiltration of AML cells into main organs. Fig. 7A shows enormous engraftment of leukemia cells in the liver of PBS group, which was progressively reduced by free Vol, PVol and TPVol treatments. In the spleen, varying degrees of heterogenic cells were observed in PBS, free Vol, PVol and TPVol groups, which could be attributed to extramedullary hematopoiesis caused by the damages in bone marrow. Besides, bleeding was detectable in the spleen of free Vol group (yellow triangles), as a result of platelet depleting effect and dose-limiting toxicity of Vol [49]. Notably, mice treated with TPVol at 9 mpk showed no visible infiltration of leukemia blasts, no tissue damage in liver, and few anomalies in spleen. It should further be noted that all Vol formulations did not cause discernible damage of heart, lung and kidney (Fig. S6).

We further determined the PLK1 and p-AKT contents in the BM of leukemic mice using western blot. Fig. 7B and C showed increasing reduction of PLK1 level from PBS, free Vol, PVol to TPVol groups, which is mostly attributable to substantially reduced infiltration of leukemic

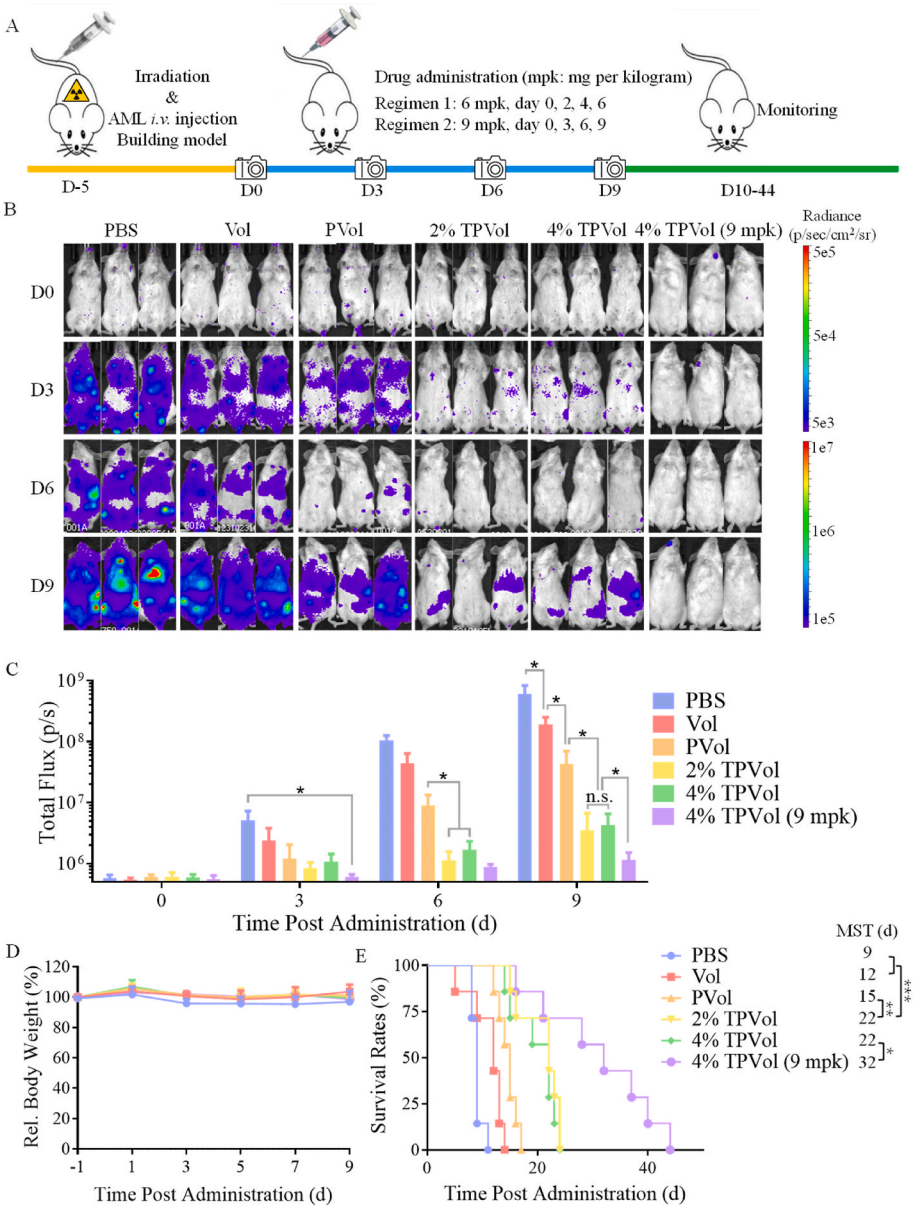

Fig. 5. *In vivo* anti-AML efficacy of TPVol, PVol, and free Vol in orthotopic MV-4-11 leukemic mouse model (n = 7). (A) Workflow for building AML model and treating with different Vol formulations. The tumor bioluminescence images (B) and quantitative bioluminescence analyses (C) of MV-4-11 leukemic mice on day 0, 3, 6 and 9 after different treatments. Statistical analysis: one-way ANOVA with Tukey multiple comparisons tests: *p < 0.05, **p < 0.01, ***p < 0.001, ****p < 0.0001. D) Relative body weight of the mice. (E) Kaplan–Meier survival curves. Statistical analysis: one-way ANOVA with Log-rank (Mantel–Cox) test, *p < 0.05.

blasts in BM. The p-AKT was more downregulated by different Vol formulations. As a matter of fact, p-AKT in PVol and TPVol groups was hardly detected (Fig. 7C). This marked reduction of p-AKT is due to combination of lessened leukemic blasts proportion in BM and effective suppression of p-AKT expression in leukemic cells by PLK1 inhibition.

To evaluate the effect of TPVol treatment to bone microenvironment, we analyzed the infiltration of osteoclasts using tartrate resistant acid phosphatase (TRAP) staining and bone damage to tibias and femurs using micro-compute tomography (μCT). TRAP images showed abundant osteoclasts (stained dark-red) in the femurs and tibias of PBS group, while little in those of TPVol groups (Fig. 8A). μCT images of tibias and femurs displayed obvious loss of trabecular structures for PBS and free Vol groups, clear improvement for PVol group, and significant recovery for two TPVol groups to similar level of healthy mice (Fig. 8B). The quantitative analyses of trabecular number (Tb.N), bone volume fraction (BV/TV), bone surface fraction (BS/BV), and trabecular spacing (Tb.sp) followed the same trend (Fig. 8C). It is worth noting that the mice treated with TPVol (9 mpk) had similar bone density as healthy mice and nearly intact trabecular tissue, in agreement with insignificant leukemia engraftment in BM and negligible osteoclast formation. These results corroborate that transferrin-guided polymersomes (TPs) can markedly augment the targetability, potency and safety of Vol to AML. The targeted nano-delivery of clinical molecular targeted drug appears to be a novel and attractive strategy to manage malignant AML.

4. Conclusion

We have demonstrated that Tf-functionalized polymersomes (TPs) enable robust loading and targeted delivery of a clinical molecular targeted drug, volasertib (Vol), to TfR-overexpressed AML cells *in vivo*, which can not only boost the specificity and anti-AML potency of Vol but also mitigate its systemic toxic effects. The therapeutic studies show that Vol-loaded TPs (TPVol) effectively deplete the leukemic cells in liver, spleen, bone marrow and peripheral blood in MV-4-11-Luc-GFP leukemic mice, leading to 2.5-fold longer median survival time than PBS with minimal bone damage. However, the AML mice were not completely cured, mainly due to remaining leukemic stem cells in the niche, which is the most important reason for AML relapse [47]. Further study may focus on co-delivery of drugs against cancer stem cells. Here, TPs are based on biodegradable polymers and with endogenous

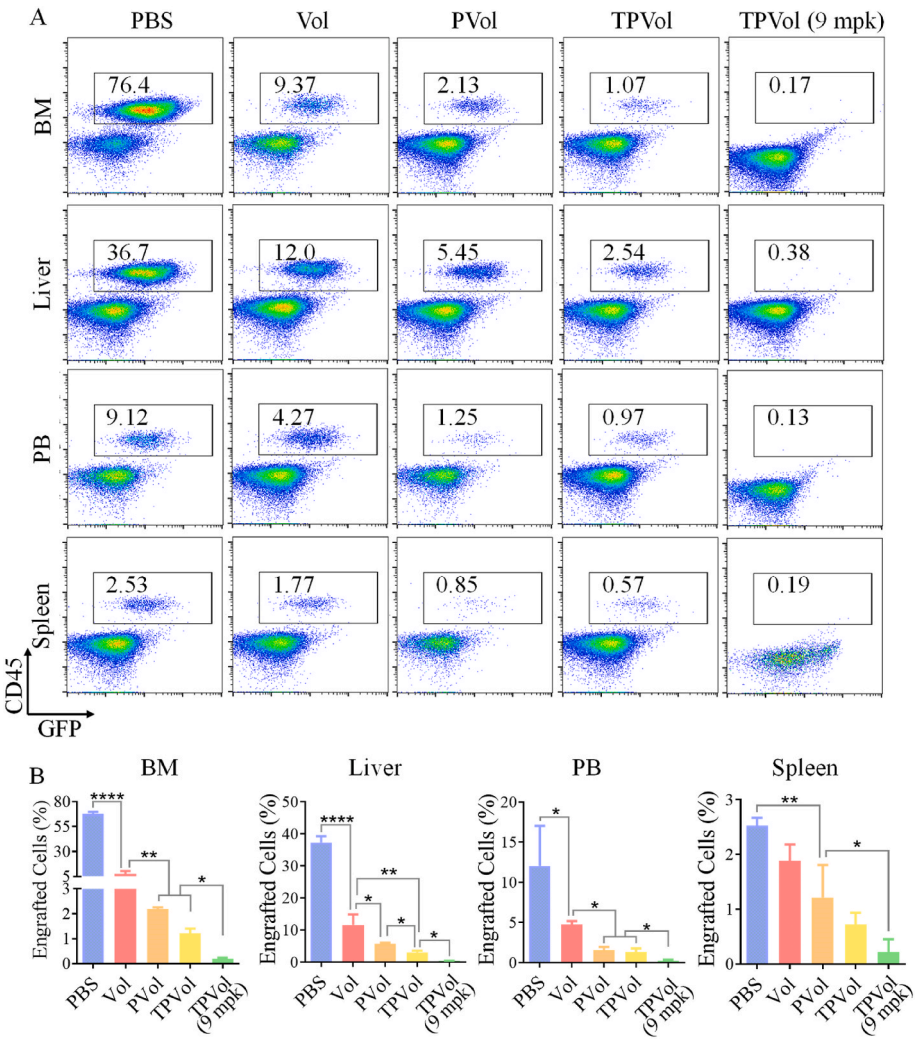

Fig. 6. The representative FACS panels (A) and quantitative analyses (B) of leukemia burden in bone marrow (BM), liver, spleen, and peripheral blood (PB) of AML mice on day 9 after different treatments. One-way ANOVA with Tukey multiple comparisons tests: *p < 0.05, **p < 0.01, ***p < 0.001, ****p < 0.0001.

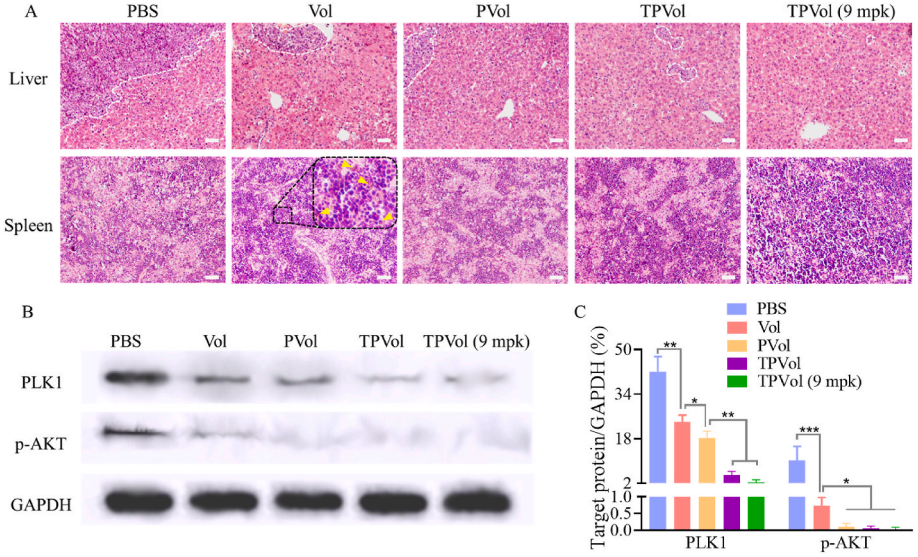

Fig. 7. *Ex vivo* evaluation of leukemia blast infiltration and PLK1 regulation. (A) Representative H&E-stained images of liver and spleen slices. Yellow triangles point to the bleeding sites. Western blot (B) and quantitative analyses (C) of the cells collected from BM on day 9 after different treatments (n = 3). Scale bar: 50 μm. One-way ANOVA with Tukey multiple comparisons tests: *p < 0.05, **p < 0.01.

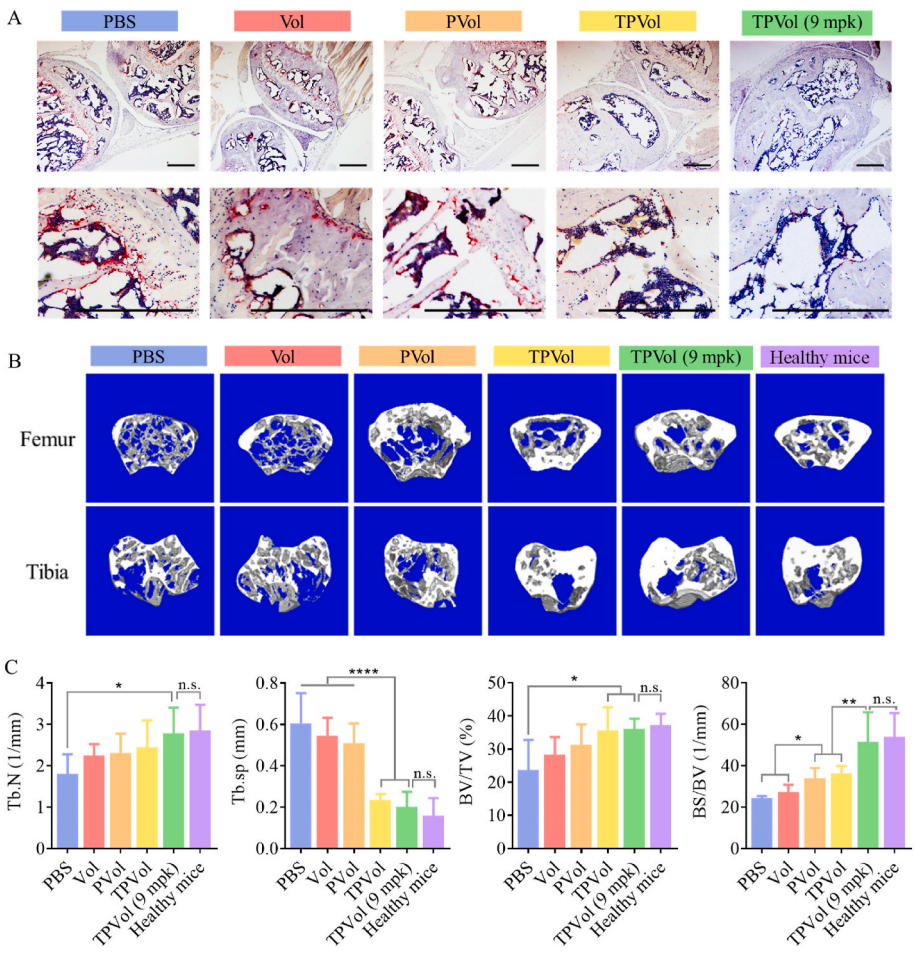

Fig. 8. Analyses of tissues of hind limbs of healthy mice and AML mice on day 9 after different treatments. (A) Representative TRAP staining images (osteoclasts: dark red). Scale bar: 200 μm. (B) μCT images and (C) quantitative analyses of tibias and femurs (n = 3). Statistics: one-way ANOVA with Tukey multiple comparisons tests: *p < 0.05, **p < 0.01, ****p < 0.0001.

transferrin as a targeting ligand, rendering it a high potential for clinical translation. This targeted nano-delivery of molecular targeted drug provides a novel and unique strategy to combat AML.

Ethics approval and consent to participate

This study received approval from the ethics committee of the First Affiliated Hospital of Soochow University (Suzhou, P. R. China) (No. 2017169-2) and was conducted according to the principles of the Declaration of Helsinki. Informed consent was obtained from all participants.

CRediT authorship contribution statement

Yifeng Xia: Methodology, Investigation, Validation, Writing – original draft. **Jingnan An:** Investigation, Validation, Data curation. **Jiaying Li:** Investigation, Data curation. **Wenxing Gu:** Methodology, Validation. **Yifan Zhang:** Methodology, Validation. **Songsong Zhao:** Investigation. **Cenzhu Zhao:** Investigation. **Yang Xu:** Resources, Supervision. **Bin Li:** Resources. **Zhiyuan Zhong:** Conceptualization, Supervision, Writing – review & editing. **Fenghua Meng:** Conceptualization, Supervision, Writing – review & editing.

Declaration of competing interest

The authors declare that they have no known competing financial interests or personal relationships that could have appeared to influence the work reported in this paper.

Acknowledgements

This work is supported by research grants from the National Natural Science Foundation of China (NSFC 52033006 and 82000157) and the Natural Science Foundation of Jiangsu Province (NO. BK20190173).

Appendix A. Supplementary data

Supplementary data to this article can be found online at https://doi.org/10.1016/j.bioactmat.2022.08.032.

References

[1] R.L. Siegel, K.D. Miller, A. Jemal, Cancer statistics, 2020, CA Cancer J. Clin. 70 (2020) 7–30, https://doi.org/10.3322/caac.21590.
[2] D.G.J. Cucchi, T.B. Polak, G.J. Ossenkoppele, C.A. Uyl–De Groot, J. Cloos, S. Zweegman, J.J.W.M. Janssen, Two decades of targeted therapies in acute myeloid leukemia, Leukemia 35 (2021) 651–660, https://doi.org/10.1038/s41375-021-01164-x.
[3] S. Horibata, G. Gui, J. Lack, C.B. DeStefano, M.M. Gottesman, C.S. Hourigan, Heterogeneity in refractory acute myeloid leukemia, P. Natl. Acad. Sci. USA 116 (2019) 10494–10503, https://doi.org/10.1073/pnas.1902375116.
[4] G. Maschmeyer, J. De Greef, S.C. Mellinghoff, A. Nosari, A. Thiebaut-Bertrand, A. Bergeron, T. Franquet, N.M.A. Blijlevens, J.A. Maertens, Infections associated with immunotherapeutic and molecular targeted agents in hematology and oncology. A position paper by the European Conference on Infections in Leukemia (ECIL), Leukemia 33 (2019) 844–862, https://doi.org/10.1038/s41375-019-0388-x.

[5] L. Zhong, Y. Li, L. Xiong, W. Wang, M. Wu, T. Yuan, W. Yang, C. Tian, Z. Miao, T. Wang, S. Yang, Small molecules in targeted cancer therapy: advances, challenges, and future perspectives, Signal Transduct. Targeted Ther. 6 (2021) 201, https://doi.org/10.1038/s41392-021-00572-w.
[6] E. Le Rhun, M. Preusser, P. Roth, D.A. Reardon, M. van den Bent, P. Wen, G. Reifenberger, M. Weller, Molecular targeted therapy of glioblastoma, Cancer Treat Rev. 80 (2019), 101896, https://doi.org/10.1016/j.ctrv.2019.101896.
[7] M. Konopleva, G. Martinelli, N. Daver, C. Papayannidis, A. Wei, B. Higgins, M. Ott, J. Mascarenhas, M. Andreeff, MDM2 inhibition: an important step forward in cancer therapy, Leukemia 34 (2020) 2858–2874, https://doi.org/10.1038/s41375-020-0949-z.
[8] A.G. Renner, C. Dos Santos, C. Recher, C. Bailly, L. Créancier, A. Kruczynski, B. Payrastre, S. Manenti, Polo-like kinase 1 is overexpressed in acute myeloid leukemia and its inhibition preferentially targets the proliferation of leukemic cells, Blood 114 (2009) 659–662, https://doi.org/10.1182/blood-2008-12-195867.
[9] A.M. Zeidan, M. Ridinger, T.L. Lin, P.S. Becker, G.J. Schiller, P.A. Patel, A.I. Spira, M.L. Tsai, E. Samuëlsz, S.L. Silberman, M. Erlander, E.S. Wang, A phase Ib study of Onvansertib, a novel oral PLK1 inhibitor, in combination therapy for patients with relapsed or refractory acute myeloid leukemia, Clin. Cancer Res. 26 (2020) 6132–6140, https://doi.org/10.1158/1078-0432.CCR-20-2586.
[10] H. Döhner, A. Symeonidis, D. Deeren, J. Demeter, M.A. Sanz, A. Anagnostopoulos, J. Esteve, W. Fiedler, K. Porkka, H.-J. Kim, J.-H. Lee, K. Usuki, S. D'Ardia, C. Won Jung, O. Salamero, H.-A. Horst, C. Recher, P. Rousselot, I. Sandhu, K. Theunissen, F. Thol, K. Döhner, V. Teleanu, D.J. DeAngelo, T. Naoe, M.A. Sekeres, V. Belsack, M. Ge, T. Taube, O.G. Ottmann, Adjunctive volasertib in patients with acute myeloid leukemia not eligible for standard induction therapy: a randomized, phase 3 trial, Hemasphere 5 (2021) e617, https://doi.org/10.1097/HS9.0000000000000617.
[11] P. Bose, S. Grant, Orphan drug designation for pracinostat, volasertib and alvocidib in AML, Leuk. Res. 38 (2014) 862–865, https://doi.org/10.1016/j.leukres.2014.06.007.
[12] J. Maertens, M. Lubbert, W. Fiedler, L. Fouillard, A. Haaland, J.M. Brandwein, S. p. Lepretre, O.d. Reman, P. Turlure, G. Bug, C. Muller-Tidow, A. Kramer, F. Voss, T. Taube, H. Fritsch, H. Dohner, Phase I/II study of volasertib (BI 6727), an intravenous polo-Like kinase (Plk) inhibitor, in patients with acute myeloid leukemia (AML): results from the randomized phase II part for Volasertib in combination with low-dose Cytarabine (LDAC) versus LDAC monotherapy in patients with previously untreated AML ineligible for intensive treatment, Blood 120 (2012) 411, https://doi.org/10.1182/blood.V120.21.411.411.
[13] Y. Kobayashi, T. Yamauchi, H. Kiyoi, T. Sakura, T. Hata, K. Ando, A. Watabe, A. Harada, T. Taube, Y. Miyazaki, T. Naoe, Phase I trial of volasertib, a polo-like kinase inhibitor, in Japanese patients with acute myeloid leukemia, Cancer Sci. 106 (2015) 1590–1595, https://doi.org/10.1111/cas.12814.
[14] W. Gu, F. Meng, R. Haag, Z. Zhong, Actively targeted nanomedicines for precision cancer therapy: concept, construction, challenges and clinical translation, J. Contr. Release 329 (2021) 676–695, https://doi.org/10.1016/j.jconrel.2020.10.003.
[15] R. van der Meel, E. Sulheim, Y. Shi, F. Kiessling, W.J.M. Mulder, T. Lammers, Smart cancer nanomedicine, Nat. Nanotechnol. 14 (2019) 1007–1017, https://doi.org/10.1038/s41565-019-0567-y.
[16] W. Gu, R. Qu, F. Meng, J.J.L.M. Cornelissen, Z. Zhong, Polymeric nanomedicines targeting hematological malignancies, J. Contr. Release 337 (2021) 571–588, https://doi.org/10.1016/j.jconrel.2021.08.001.
[17] N. Senzer, J. Nemunaitis, D. Nemunaitis, C. Bedell, G. Edelman, M. Barve, R. Nunan, K.F. Pirollo, A. Rait, E.H. Chang, Phase I study of a systemically delivered p53 nanoparticle in advanced solid tumors, Mol. Ther. 21 (2013) 1096–1103, https://doi.org/10.1038/mt.2013.32.
[18] X. Huang, S. Schwind, B. Yu, R. Santhanam, H. Wang, P. Hoellerbauer, A. Mims, R. Klisovic, A.R. Walker, K.K. Chan, W. Blum, D. Perrotti, J.C. Byrd, C. D. Bloomfield, M.A. Caligiuri, R.J. Lee, R. Garzon, N. Muthusamy, L.J. Lee, G. Marcucci, Targeted delivery of microRNA-29b by transferrin-conjugated anionic lipopolyplex nanoparticles: a novel therapeutic strategy in acute myeloid leukemia, Clin. Cancer Res. 19 (2013) 2355–2367, https://doi.org/10.1158/1078-0432.CCR-12-3191.
[19] Z. Wang, S. Zhao, W. Gu, Y. Dong, F. Meng, J. Yuan, Z. Zhong, α3 integrin-binding peptide-functionalized polymersomes loaded with volasertib for dually-targeted molecular therapy for ovarian cancer, Acta Biomater. 124 (2021) 348–357, https://doi.org/10.1016/j.actbio.2021.02.007.
[20] C. Zhou, Y.F. Xia, Y.H. Wei, L. Cheng, J.J. Wei, B.B. Guo, F.H. Meng, S.P. Cao, J.C. M. van Hest, Z.Y. Zhong, GE11 peptide-installed chimaeric polymersomes tailor-made for high-efficiency EGFR-targeted protein therapy of orthotopic hepatocellular carcinoma, Acta Biomater. 113 (2020) 512–521, https://doi.org/10.1016/j.actbio.2020.06.020.
[21] N. Yu, Y.F. Zhang, J.Y. Li, W.X. Gu, S.J. Yue, B. Li, F.H. Meng, H.L. Sun, R. Haag, J. D. Yuan, Z.Y. Zhong, Daratumumab immunopolymersome-enabled safe and CD38-targeted chemotherapy and depletion of multiple myeloma, Adv. Mater. 33 (2021), 2007787, https://doi.org/10.1002/adma.202007787.
[22] A.L. Kampmann, T. Grabe, C. Jaworski, R. Weberskirch, Synthesis of well-defined core-shell nanoparticles based on bifunctional poly(2-oxazoline) macromonomer surfactants and a microemulsion polymerization process, RSC Adv. 6 (2016) 99752–99763, https://doi.org/10.1039/c6ra22896h.
[23] Y. Xia, J. Wei, S. Zhao, B. Guo, F. Meng, B. Klumperman, Z. Zhong, Systemic administration of polymersomal oncolytic peptide LTX-315 combining with CpG adjuvant and anti-PD-1 antibody boosts immunotherapy of melanoma, J. Contr. Release 336 (2021) 262–273, https://doi.org/10.1016/j.jconrel.2021.06.032.
[24] W.X. Gu, J.N. An, H. Meng, N. Yu, Y.N. Zhong, F.H. Meng, Y. Xu, J.J.L. M. Cornelissen, Z.Y. Zhong, CD44-specific A6 short peptide boosts targetability and anticancer efficacy of polymersomal epirubicin to orthotopic human multiple myeloma, Adv. Mater. 31 (2019), 1904742, https://doi.org/10.1002/adma.201904742.
[25] K.F. Pirollo, J. Nemunaitis, P.K. Leung, R. Nunan, J. Adams, E.H. Chang, Safety and efficacy in advanced solid tumors of a targeted nanocomplex carrying the p53 gene used in combination with docetaxel: a phase 1b study, Mol. Ther. 24 (2016) 1697–1706, https://doi.org/10.1038/mt.2016.135.
[26] A. Siefker-Radtke, X.-q. Zhang, C.C. Guo, Y. Shen, K.F. Pirollo, S. Sabir, C. Leung, C. Leong-Wu, C.-M. Ling, E.H. Chang, R.E. Millikan, W.F. Benedict, A phase l study of a tumor-targeted systemic nanodelivery system, SGT-94, in genitourinary cancers, Mol. Ther. 24 (2016) 1484–1491, https://doi.org/10.1038/mt.2016.118.
[27] P. Kollia, N. Stavroyianni, K. Stamatopoulos, K. Zoi, N. Viniou, M. Mantzourani, C. T. Noguchi, G. Paterakis, D. Abazis, C. Pangalos, D. Loukopoulos, X. Yataganas, Molecular analysis of transferrin receptor mRNA expression in acute myeloid leukaemia, Br. J. Haematol. 115 (2001) 19–24, https://doi.org/10.1046/j.1365-2141.2001.03065.x.
[28] C.H.J. Choi, C.A. Alabi, P. Webster, M.E. Davis, Mechanism of active targeting in solid tumors with transferrin-containing gold nanoparticles, P. Natl. Acad. Sci. USA 107 (2010) 1235–1240, https://doi.org/10.1073/pnas.0914140107.
[29] Y. Wei, X. Gu, L. Cheng, F. Meng, G. Storm, Z. Zhong, Low-toxicity transferrin-guided polymersomal doxorubicin for potent chemotherapy of orthotopic hepatocellular carcinoma in vivo, Acta Biomater. 92 (2019) 196–204, https://doi.org/10.1016/j.actbio.2019.05.034.
[30] W.T. Weng Ng, J.-S. Shin, T.L. Roberts, B. Wang, C.S. Lee, Molecular interactions of polo-like kinase 1 in human cancers, J. Clin. Pathol. 69 (2016) 557–562, https://doi.org/10.1136/jclinpath-2016-203656.
[31] L. Gheghiani, D. Loew, B. Lombard, J. Mansfeld, O. Gavet, PLK1 activation in late G2 sets up commitment to mitosis, Cell Rep. 19 (2017) 2060–2073, https://doi.org/10.1016/j.celrep.2017.05.031.
[32] S.K. Cimino, C. Eng, Up-and-coming experimental drug options for metastatic colorectal cancer, J. Exp. Pharmacol. 12 (2020) 475–485, https://doi.org/10.2147/JEP.S259287.
[33] E. Montaudon, J. Nikitorowicz-Buniak, L. Sourd, L. Morisset, R. El Botty, L. Huguet, A. Dahmani, P. Painsec, F. Nemati, S. Vacher, W. Chemlali, J. Masliah-Planchon, S. Château-Joubert, C. Rega, M.F. Leal, N. Simigdala, S. Pancholi, R. Ribas, A. Nicolas, D. Meseure, A. Vincent-Salomon, C. Reyes, A. Rapinat, D. Gentien, T. Larcher, M. Bohec, S. Baulande, V. Bernard, D. Decaudin, F. Coussy, M. Le Romancer, G. Dutertre, Z. Tariq, P. Cottu, K. Driouch, I. Bièche, L.-A. Martin, E. Marangoni, PLK1 inhibition exhibits strong anti-tumoral activity in CCND1 -driven breast cancer metastases with acquired palbociclib resistance, Nat. Commun. 11 (2020) 4053, https://doi.org/10.1038/s41467-020-17697-1.
[34] J. Li, R. Wang, Y. Kong, M.M. Broman, C. Carlock, L. Chen, Z. Li, E. Farah, T. L. Ratliff, X. Liu, Targeting Plk1 to enhance efficacy of olaparib in castration-resistant prostate cancer, Mol. Cancer Therapeut. 16 (2017) 469–479, https://doi.org/10.1158/1535-7163.MCT-16-0361.
[35] Z. Gao, X. Man, Z. Li, J. Bi, X. Liu, Z. Li, J. Li, Z. Zhang, C. Kong, PLK1 promotes proliferation and suppresses apoptosis of renal cell carcinoma cells by phosphorylating MCM3, Cancer Gene Ther. 27 (2020) 412–423, https://doi.org/10.1038/s41417-019-0094-x.
[36] A.M. Zeidan, M. Ridinger, T.L. Lin, P.S. Becker, G.J. Schiller, P.A. Patel, A.I. Spira, M.L. Tsai, E. Samuëlsz, S.L. Silberman, M. Erlander, E.S. Wang, A phase Ib study of Onvansertib, a novel oral PLK1 inhibitor, in combination therapy for patients with relapsed or refractory acute myeloid leukemia, Clin. Cancer Res. 26 (2020) 6132–6140, https://doi.org/10.1158/1078-0432.CCR-20-2586.
[37] H. Gibori, S. Eliyahu, A. Krivitsky, D. Ben-Shushan, Y. Epshtein, G. Tiram, R. Blau, P. Ofek, J.S. Lee, E. Ruppin, L. Landsman, I. Barshack, T. Golan, E. Merquiol, G. Blum, R. Satchi-Fainaro, Amphiphilic nanocarrier-induced modulation of PLK1 and miR-34a leads to improved therapeutic response in pancreatic cancer, Nat. Commun. 9 (2018) 16, https://doi.org/10.1038/s41467-017-02283-9.
[38] B.T. Gjertsen, P. Schoffski, Discovery and development of the polo-like kinase inhibitor volasertib in cancer therapy, Leukemia 29 (2015) 11–19, https://doi.org/10.1038/leu.2014.222.
[39] B.H. Choi, M. Pagano, W. Dai, Plk1 protein phosphorylates phosphatase and tensin homolog (PTEN) and regulates its mitotic activity during the cell cycle, J. Biol. Chem. 289 (2014) 14066–14074, https://doi.org/10.1074/jbc.M114.558155.
[40] A.-M. Bleau, D. Hambardzumyan, T. Ozawa, E.I. Fomchenko, J.T. Huse, C. W. Brennan, E.C. Holland, PTEN/PI3K/Akt pathway regulates the side population phenotype and ABCG2 activity in glioma tumor stem-like cells, Cell Stem Cell 4 (2009) 226–235, https://doi.org/10.1016/j.stem.2009.01.007.
[41] Y. Adachi, Y. Ishikawa, H. Kiyoi, Identification of volasertib-resistant mechanism and evaluation of combination effects with volasertib and other agents on acute myeloid leukemia, Oncotarget 8 (2017) 78452–78465, https://doi.org/10.18632/oncotarget.19632.
[42] W. Gu, J. An, H. Meng, N. Yu, Y. Zhong, F. Meng, Y. Xu, J.J.L.M. Cornelissen, Z. Zhong, CD44-specific A6 short peptide boosts targetability and anticancer efficacy of polymersomal epirubicin to orthotopic human multiple myeloma, Adv. Mater. 31 (2019), 1904742, https://doi.org/10.1002/adma.201904742.
[43] D.M. Moujalled, G. Pomilio, C. Ghiurau, A. Ivey, J. Salmon, S. Rijal, S. Macraild, L. Zhang, T.-C. Teh, I.-S. Tiong, P. Lan, M. Chanrion, A. Claperon, F. Rocchetti, A. Zichi, L. Kraus-Berthier, Y. Wang, E. Halilovic, E. Morris, F. Colland, D. Segal, D. Huang, A.W. Roberts, A.L. Maragno, G. Lessene, O. Geneste, A.H. Wei, Combining BH3-mimetics to target both BCL-2 and MCL1 has potent activity in pre-clinical models of acute myeloid leukemia, Leukemia 33 (2019) 905–917, https://doi.org/10.1038/s41375-018-0261-3.
[44] M. Noviello, F. Manfredi, E. Ruggiero, T. Perini, G. Oliveira, F. Cortesi, P. De Simone, C. Toffalori, V. Gambacorta, R. Greco, J. Peccatori, M. Casucci,

G. Casorati, P. Dellabona, M. Onozawa, T. Teshima, M. Griffioen, C.J.M. Halkes, J. H.F. Falkenburg, F. Stölzel, H. Altmann, M. Bornhäuser, M. Waterhouse, R. Zeiser, J. Finke, N. Cieri, A. Bondanza, L. Vago, F. Ciceri, C. Bonini, Bone marrow central memory and memory stem T-cell exhaustion in AML patients relapsing after HSCT, Nat. Commun. 10 (2019) 1065, https://doi.org/10.1038/s41467-019-08871-1.

[45] W. Gu, T. Liu, D. Fan, J. Zhang, Y. Xia, F. Meng, Y. Xu, J.J.L.M. Cornelissen, Z. Liu, Z. Zhong, A6 peptide-tagged, ultra-small and reduction-sensitive polymersomal vincristine sulfate as a smart and specific treatment for CD44+ acute myeloid leukemia, J. Contr. Release 329 (2021) 706–716, https://doi.org/10.1016/j.jconrel.2020.10.005.

[46] Y. Shi, Z. Su, S. Li, Y. Chen, X. Chen, Y. Xiao, M. Sun, Q. Ping, L. Zong, Multistep targeted nano drug delivery system aiming at leukemic stem cells and minimal residual disease, Mol. Pharm. 10 (2013) 2479–2489, https://doi.org/10.1021/mp4001266.

[47] D.C. Johnson, C.Y. Taabazuing, M.C. Okondo, A.J. Chui, S.D. Rao, F.C. Brown, C. Reed, E. Peguero, E. de Stanchina, A. Kentsis, D.A. Bachovchin, DPP8/DPP9 inhibitor-induced pyroptosis for treatment of acute myeloid leukemia, Nat. Med. 24 (2018) 1151–1156, https://doi.org/10.1038/s41591-018-0082-y.

[48] K. Ramaswamy, L. Forbes, G. Minuesa, T. Gindin, F. Brown, M.G. Kharas, A. V. Krivtsov, S.A. Armstrong, E. Still, E. de Stanchina, B. Knoechel, R. Koche, A. Kentsis, Peptidomimetic blockade of MYB in acute myeloid leukemia, Nat. Commun. 9 (2018) 110, https://doi.org/10.1038/s41467-017-02618-6.

[49] Y. Kobayashi, T. Yamauchi, H. Kiyoi, T. Sakura, T. Hata, K. Ando, A. Watabe, A. Harada, T. Taube, Y. Miyazaki, T. Naoe, Phase I trial of volasertib, a polo-like kinase inhibitor, in Japanese patients with acute myeloid leukemia, Cancer Sci. 106 (2015) 1590–1595, https://doi.org/10.1111/cas.12814.

[50] B. Kumar, M. Garcia, L. Weng, X. Jung, J.L. Murakami, X. Hu, T. McDonald, A. Lin, A.R. Kumar, D.L. DiGiusto, A.S. Stein, V.A. Pullarkat, S.K. Hui, N. Carlesso, Y. H. Kuo, R. Bhatia, G. Marcucci, C.C. Chen, Acute myeloid leukemia transforms the bone marrow niche into a leukemia-permissive microenvironment through exosome secretion, Leukemia 32 (2018) 575–587, https://doi.org/10.1038/leu.2017.259.

[51] H. Ågerstam, C. Karlsson, N. Hansen, C. Sandén, M. Askmyr, S. von Palffy, C. Högberg, M. Rissler, M. Wunderlich, G. Juliusson, J. Richter, K. Sjöström, R. Bhatia, J.C. Mulloy, M. Järås, T. Fioretos, Antibodies targeting human IL1RAP (IL1R3) show therapeutic effects in xenograft models of acute myeloid leukemia, P. Natl. Acad. Sci. USA 112 (2015) 10786–10791, https://doi.org/10.1073/pnas.1422749112.